Journal of Sound and Vibration (1997) **208**(3), 391–406

OPTIMIZATION OF ENERGY DISSIPATION OF ACTIVE CONSTRAINED LAYER DAMPING TREATMENTS OF PLATES

M. C. Ray and A. Baz

Mechanical Engineering Department, The Catholic University of America, Washington, DC 20064, *U.S.A.*

(*Received* 1 *October* 1996, *and in final form* 30 *May* 1997)

The energy dissipation characteristics of **A**ctive **C**onstrained **L**ayer **D**amping (ACLD) treatments of plates is optimized using rational design procedures. Such treatments of plates is optimized using rational design procedures. Such treatments consist of viscoelastic cores constrained by active piezo-electric layers. The optimal size and control gains of these ACLD treatments are determined using a globally stable boundary control strategy to control the strains of the active peizo-electric layers in response to the structural vibrations. The optimal parameters are obtained to maximize the sum of the passive and active loss coefficients of the ACLD treatments. The effect of the viscoelastic loss factor as well as the aspect ratio and piezo-electrical anisotropy of the constraining layer on the performance and the optimal parameters of the ACLD treatments is determined. Comparisons with optimal **P**assive **C**onstrained **L**ayer **D**amping (PCLD) indicate that the optimal ACLD is more effective in dissipating vibrational energy.

1. INTRODUCTION

Considerable interest has been devoted to the development, modeling and testing of ACLD treatments of flexible structures because of their effectiveness of damping out structural vibrations [1–16]. In this class of damping treatments, viscoelastic damping layers are constrained by active piezo-electric layers whose longitudinal strains are controlled in response to the structural vibrations in order to enhance the energy dissipation characteristics. Recently, attempts have been made to optimize the performance of the ACLD treatments by selecting the optimal thickness and shear modulus of the viscoelastic cores as well as the control gains for fully-treated beams when proportional and derivative controllers are used [13, 17]. Baz [5] developed the optimal length and control gains for ACLD treatments of beam-type structures by maximizing the sum of the passive and active loss coefficients. His analysis was an extension of the pioneering work of Plunkett and Lee [18] for determining the optimal length of PCLD treatments of beams.

In the present study, the emphasis is placed on extending the work of Baz [5] to determine the optimal size and control gains of plate-type ACLD treatments using globally stable boundary controllers.

This paper is organized in seven sections. In section 1 a brief introduction is given. The concept of the active constrained layer damping is presented in section 2. The theories governing the operation of the ACLD and the globally stable boundary controller are described in sections 3 and 4. The energy dissipation of the ACLD is quantified in section

0022–460X/97/480391 + 16 $25.00/0/sv971171

5 and optimized in section 6. In section 6, numerical examples are also presented to compare the performance of the optimal ACLD treatment with those of conventional PCLD. Section 7 gives a brief summary of the conclusions.

2. THE CONCEPT OF THE ACTIVE CONSTRAINED LAYER DAMPING

The ACLD treatment consists of a viscoelastic constrained layer and a piezo-electric layer, acting as active constraining layer and is augmented with efficient *active* control means to control the strain of the constraining layer, in response to the structural vibrations. The two-layer composite ACLD when bonded to the base structure acts as a smart constrained layer damping treatment with built-in control capabilities. In practice the constrained layer damping treatment is periodically cut into several segments in order to optimize the effectiveness of the damping treatment on a large structure [18, 19]. Such a typical segment of ACLD treatment on a plate is shown in Figures 1 and 2. When the base structure experiences the longitudinal displacements, u_0 and v_0 at the interface between it and the viscoelastic core in the x and y directions, respectively, the in-active constraining layer undergoes the corresponding displacements u_{pa} and v_{pa} at the interface between it and viscoelastic core. Consequently, the viscoelastic layer is subjected to a passive shear stain, γ_{pa}, in the x-z plane as shown in Figure 2(b). Under these conditions, the ACLD acts as a conventional PCLD. But, when the constraining layer is activated properly by the controller, the passive displacements u_{pa} and v_{pa} change to u and v, respectively. Thus an additional displacement $(u - u_p)$ is generated by the piezo-electric effect to increase the shear strain of the viscoelastic core to γ_1 as shown in Figure 2(c) in the x-z plane. The corresponding increase in the shear strain $(\gamma_1 - \gamma_{pa})$ enhances the energy dissipation characteristics of the ACLD and results in effective damping of the structural vibrations. Similarly, the activated piezo-layer also undergoes an additional deflection $(v - v_{pa})$ in the y direction resulting in increasing the shear strain of the viscoelastic core in the y-z plane to γ_2.

3. VARIATIONAL MODELLING OF ACTIVE CONSTRAINED LAYER DAMPING TREATMENT OF PLATES

3.1. OVERVIEW

A distributed parameter model is developed using Hamilton's principle to describe the behavior of ACLD treatments of plates. The model is an extension to the beam model

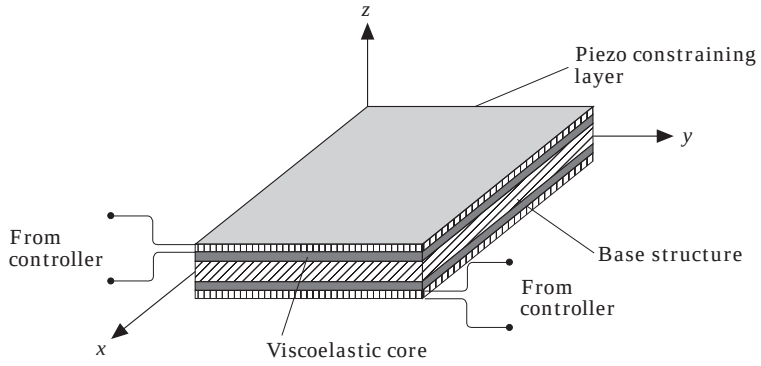

Figure 1. Schematic diagram of the active constrained layer damping

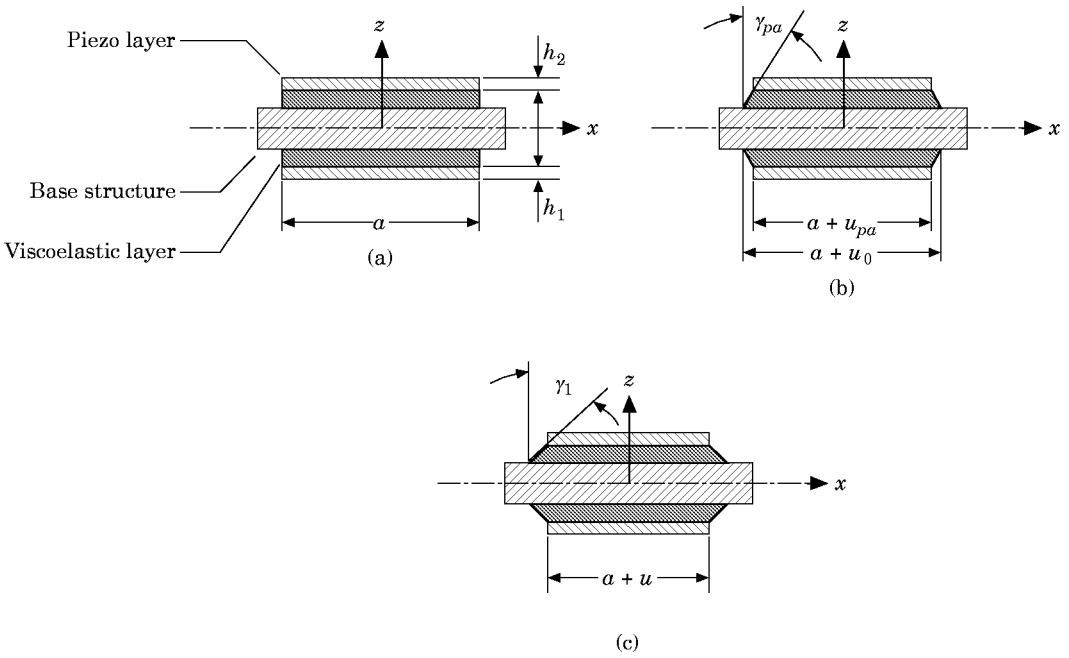

Figure 2. Operating principles of the PCLD and the ACLD treatments: (a) undeformed, (b) PCLD, (c) ACLD.

of PCLD developed by Plunkett and Lee [18] and of ACLD developed by Baz [5]. The variational model is utilized as a basis for devising a globally stable boundary control strategy which is compatible with the operating nature of the ACLD treatments. In this manner, the instability problems associated with the simple proportional and/or derivative controllers are completely avoided. Furthermore, as the control strategy is based on distributed parameter model, the classical spillover problems resulting from using "truncated" finite element models are eliminated. Accordingly, the devised boundary controller will be able to control all the modes of vibration of the ACLD treated structures.

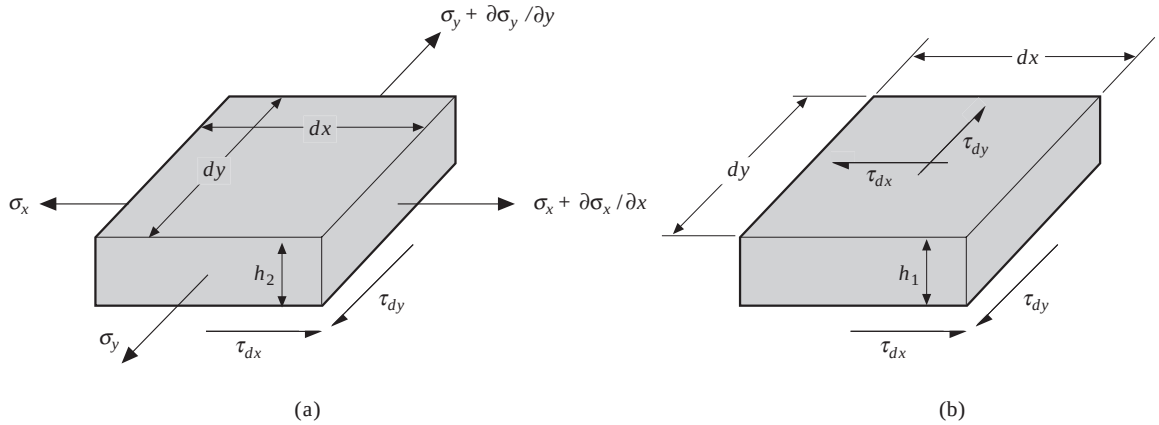

Figure 3. Schematic freebody diagram of the ACLD treatment: (a) piezo constraining layer, (b) visco-elastic layer.

3.2. MAIN ASSUMPTIONS OF THE MODEL

Figure 3 shows a schematic free body diagram of the ACLD treatment. It is assumed that the thicknesses of the piezo-constraining and viscoelastic layers are very small compared to that of the base structure. Hence, the bending effects are negligible, the constraining layer is subjected to in-plane strains only and the viscoelastic core is subjected to shear only. The piezo-electric constraining layer is assumed to be elastic and dissipate no energy whereas the core is assumed to be linearly viscoelastic. It is also assumed that the longitudinal stresses in the viscoelastic core are negligible. Furthermore, the shear stress in the viscoelastic layer and the stresses in the constraining layer are assumed to be uniform through their thickness. In addition, the base strucure is subjected to longitudinal strains ε_{0x} and ε_{0y} in the x and y directions, respectively, which are assumed to be spatially uniform over the interface of the base structure and viscoelastic layer and temporally varying in a sinusiodal manner at a frequency, ω, due to cyclic vibration of the base structure. It may be noted that the above assumptions are consistent with those made by Plunkett and Lee [18] and Baz [5].

3.3. KINEMATIC RELATIONSHIPS

From the geometry of Figure 2 along with the concept of active constrained layer damping, the shear strains, γ_1 and γ_2 in the viscoelastic core due to the effects of piezo-constraining layer and the deformations of the base structure in the x and y directions, respectively, can be expressed as

$$\gamma_1 = (u - u_0)/h_1, \qquad \gamma_2 = (v - v_0)/h_1, \tag{1}$$

in which h_1 denotes the thickness of the viscoelastic layer.

3.4. ENERGIES OF AN ACLD SYSTEM

3.4.1. *Potential Energies*

The potential energies, U_1 and U_2 associated with the plane stress deformations of the piezo-electric constraining layer and the shearing of the viscoelastic layer of the ACLD system, respectively, are

$$U_1 = \tfrac{1}{2} h_2 \int_{-b/2}^{b/2} \int_{-a/2}^{a/2} [C_{11} u_x^2 + 2C_{12} u_x v_y + C_{22} v_y^2 + C_{66} (u_y + v_x)^2 \, \mathrm{d}x \, \mathrm{d}y, \tag{2}$$

and

$$U_2 = \tfrac{1}{2} G' h_1 \int_{-b/2}^{b/2} \int_{-a/2}^{a/2} (\gamma_1^2 + \gamma_2^2) \, \mathrm{d}x \, \mathrm{d}y, \tag{3}$$

where C_{11}, C_{22}, C_{12}, and C_{66} are the elastic constants of the piezo-layer, h_2; a and b are its thickness, length and width, respectively. The subscripts x and y denote partial differentiation with respect to x and y, respectively. Also, h_1 is the thickness of the viscoelastic layer. In equation (3), it is assumed that the behaviour of the viscoelastic layer is linear and described in terms of the complex modulus $G^* = G'(1 + \eta_g \, \mathrm{i})$ with G', η_g and i denoting the storage shear modulus, loss factor and $\sqrt{-1}$, respectively.

3.4.2. *Kinetic Energy*

The kinetic energy T associated with the longitudinal displacements u and v is given by

$$T = \tfrac{1}{2}\,\mathrm{mb}\int_{-b/2}^{b/2}\int_{-a/2}^{a/2}(u_t^2 + v_t^2)\,\mathrm{d}x\,\mathrm{d}y, \tag{4}$$

where m is the mass per unit area of the piezo-electric constraining layer and the subscript t denotes differentiation with respect to time. In equation (4), the rotary inertia of the viscoelastic layer is neglected and also the inertia of the base structure is not considered.

3.5. WORK DONE IN AN ACLD SYSTEM

The work done, W_1, by the piezo-electric control forces is given by

$$W_1 = \int_{-b/2}^{b/2}\int_{-a/2}^{a/2} -h_2\left\{(C_{11}\,\varepsilon_{px} + C_{12}\,\varepsilon_{py})u_x + (C_{12}\,\varepsilon_{px} + C_{22}\,\varepsilon_{py})v_y\right\}\mathrm{d}x\,\mathrm{d}y, \tag{5}$$

where ϵ_{px} and ϵ_{py} are the strains induced in the piezo-electric constraining layer due to the applied control voltage in response to longitudinal displacements in the x and y directions, respectively. In this study, these strains are assumed to be spatially constant at any instant in order to maintain and emphasize the simplicity and practicality of the ACLD treatment.

Note that due to the particular nature of the piezo-film which allows it only to induce in-plane longitudinal strains, the inplane shear strain ε_{pxy} is not considered in equation (5).

The work W_2 dissipated in the viscoelastic core is given by

$$W_2 = -h_1\int_{-b/2}^{b/2}\int_{-a/2}^{a/2}(\tau_{\mathrm{d}x}\,\gamma_1 + \tau_{\mathrm{d}y}\,\gamma_2)\,\mathrm{d}x\,\mathrm{d}y, \tag{6}$$

where τ_{dx} and τ_{dy} are the dissipative shear stresses developed in the viscoelastic core. These are given by

$$[\tau_{\mathrm{d}x}\ \tau_{\mathrm{d}y}] = (G'\eta_g/\omega)\,[\gamma_{1t}\ \gamma_{2t}] = (G'\eta_g\,\mathrm{i})\,[\gamma_1\ \gamma_2]. \tag{7}$$

In equation (7), the behaviour of the viscoelastic core is modelled using the common complex modulus approach which is a frequency domain-based method [20]. Adoption of this approach results in a variational model of the ACLD which can be easily reduced to the classical models of Plunkett and Lee [18] when the piezo-electric strain, ε_{px}, is set equal to zero. However, other viscoelastic models such as the Golla–Hughes–McTavish (GHM) method are being considered as viable means for describing the transient behavior of the ACLD [21].

3.6. THE MODEL

The equations and boundary conditions governing the operation of the ACLD system are obtained by applying Hamilton's principle [22],

$$\int_{t_1}^{t_2}\delta\left(T - \sum_{i=1}^{2} U_i\right)\mathrm{d}t + \int_{t_1}^{t_2}\delta\left(\sum_{j=1}^{2} W_j\right)\mathrm{d}t = 0, \tag{8}$$

where $\delta(\cdot)$ denotes the first variation in the quantity inside the parentheses. Also, t denotes time with t_1 and t_2 defining the integration time limits. Using equations (1)–(7) in equation (8), the following equations of the ACLD system are obtained:

$$mh_1/G^* u_{tt} = B_x^{*2} u_{xx} + B_{xy}^{*2} v_{xy} + B_z^{*2} u_{yy} - (u - u_0), \tag{9}$$

$$mh_1/G^* v_{tt} = B_z^{*2} v_{xx} + B_{xy}^{*2} u_{xy} + B_y^{*2} v_{yy} - (v - v_0), \tag{10}$$

along with the boundary conditions

$$u_x = \varepsilon_{px}, \text{ at } x = \pm a/2; \qquad v_y = \varepsilon_{py} \text{ at } y = \pm b/2; \tag{11a}$$

$$u_y + v_x = 0 \text{ at } x = \pm a/2, \; y = \pm b/2, \tag{11b}$$

where

$$B_x^* = \sqrt{h_1 h_2 C_{11}/G^*}, \qquad B_y^* = \sqrt{h_1 h_2 C_{22}/G^*}, \qquad B_z^* = \sqrt{h_1 h_2 C_{66}/G^*}$$

$$B_{xy}^* = \sqrt{h_1 h_2 (C_{12} + C_{66})/G^*}.$$

It is important here to note that the second order partial differential equation describing the ACLD system dynamics in the x direction (equation (9)) is the same as that describing conventional PCLD as obtained by Plunkett and Lee [18] if the inertia of the constraining layer is set to zero. However, the boundary conditions given by equation (11) are in a modified form to account for the control actions generated by the strains, ε_{px} and ε_{py}, induced by the active constraining layer at the free ends of the constraining layer (i.e., at $x = \pm a/2$ and $y = \pm b/2$).

Therefore, the particular nature of operation of the ACLD system implies that existence of boundary control actions ε_{px} and ε_{py}. In section 4, a boundary control strategy is devised to capitalize on this inherent operating nature of the ACLD system in such a manner that ensures global stability of all the vibration modes of the system.

4. BOUNDARY CONTROL STRATEGY

4.1. OVERVIEW

Distributed parameter control theory [23] is used to devise a boundary control strategy that generates the boundary control actions, ε_{px} and ε_{py}, in order to ensure global stability of all the vibration modes of the ACLD system. The control strategy is devised to ensure that the total energy of the ACLD system is a strictly non-increasing function of time. In this regard, the approach adopted here is similar to that reported by Baz [5, 7, 8] and Shen [24].

4.2. CONTROL STRATEGIES

The total energy, E_n of the ACLD system is obtained using equations (1) through (7) as follows:

$$E_n = U_1 + U_2 + T$$

or

$$E_n = \tfrac{1}{2} \int_{-b/2}^{b/2} \int_{-a/2}^{a/2} [h_2 \{C_{11} u_x^2 + 2C_{12} u_x v_y + C_{22} v_y^2 + (C_{12} + C_{66})(u_y + v_x)^2\}$$

$$+ G' h_1 (\gamma_1^2 + \gamma_2^2) + m(u_t^2 + v_t^2)] \, \mathrm{d}x \, \mathrm{d}y. \tag{12}$$

Equation (12) gives the energy norm of the ACLD system. This norm is equal to zero if and only if (u, u_t) and (v, v_t) are zeros at all points along the length and breadth of the constraining layer. This condition is ensured only when the ACLD system reverts back to its original undeflected equilibrium position.

Differentiating equation (12) with respect to time, integrating by parts and using equations (9) and (10) the following equation is obtained:

$$\dot{E}_n = \int_{-b/2}^{b/2} h_2 (C_{11}\,\varepsilon_{px} + C_{12}\,\varepsilon_{py})\{u_t\,(a/2) - u_t\,(-a/2)\}\,\mathrm{d}y$$

$$+ \int_{-a/2}^{a/2} h_2 (C_{12}\,\varepsilon_{px} + C_{22}\,\varepsilon_{py})\{v_t\,(b/2) - v_t\,(-b/2)\}\,\mathrm{d}x$$

$$- (G'\eta_g\,h_1\,/\omega) \int_{-a/2}^{a/2} \int_{-b/2}^{b/2} (\gamma_1^2 + \gamma_2^2)\,\mathrm{d}x\,\mathrm{d}y \tag{13}$$

In the above equation the first and third terms define the energy dissipation rate due to the active control actions (ε_{px} and ε_{py}) whereas the second term defines the corresponding contribution due to the passive damping generated by the viscoelastic core. Note that the second term is strictly negative indicating that the passive damping provides inherently a stabilizing effect to the plate system. As for the sum of the first and third terms, it can be rendered to be strictly negative to stabilize the active control actions if the control strains ε_{px} and ε_{py} are selected properly. We have to note, in this regard, the particular operating nature of the piezo-constraining layer which makes any control voltage applied across the layer thickness, i.e., in the z direction, generate in-plane strains in both the x and y directions. Thus, the control action is coupled in nature and the piezo-strains, ε_{px} and ε_{py}, are not independent but are related by

$$\varepsilon_{py} = (d_{32}/d_{31})\varepsilon_{px}, \tag{14}$$

where d_{31} and d_{32} are the piezo-strain contants which quantify the strains in the x and y directions (1 and 2) due to the applied electric field in the z direction (3). Hence, in order to guarantee that the energy norm will be continuously decreasing, the control action, ε_{px} should take the form

$$\varepsilon_{px} = -\left[K_x \int_{-b/2}^{b/2} \{u_t\,(a/2) - u_t\,(-a/2)\}\,\mathrm{d}y + K_y \int_{-a/2}^{a/2} \{v_t\,(b/2) - v_t\,(-b/2)\}\,\mathrm{d}x\right], \tag{15}$$

provided that

$$K_y\,/\mathrm{K}_x = (C_{12} + (d_{32}\,/d_{31})C_{22})/(C_{11} + (d_{32}\,/d_{31})C_{12}), \tag{16}$$

where, K_x and K_y are the control gains of the boundary controller.

Equations (14) and (15) indicate that the control actions are the integral effect of feedback of differential velocities at the boundaries of the piezo-electric constraining layer. It is also important here to note that when the active control actions ε_{px} and ε_{py} cease or fail to operate for one reason or another (i.e., when $\varepsilon_{px} = 0$ and $\varepsilon_{py} = 0$), the plate system remains globally stable as indicated by equation (13). Such inherent stability is attributed to the second term of the equation which quantifies the contribution of the PCLD. Hence, equation (13) provides quantitative means for weighing the individual contributions of the ACLD and the PCLD to the total rate of energy dissipation of the base structure.

4.3. IMPLEMENTATION OF THE BOUNDARY CONTROLLERS

The globally stable boundary controller can be easily implemented by solving the partial differential equations (9) and (10) subject to the boundary conditions given by equations (11a) and (11b). Since the actuating strains (ε_{px} and ε_{py}) at any instant are constants along the boundaries (equation (11a)), the displacement functions u and v cannot satisfy equations (11a) and (11b) unless u is function x and v is function of y only. Thus the analysis is a particular case of axisymmetric vibration in a plane. Hence using the approach adopted by Plunkett and Lee [18] for the case of PCLD treatments where the effect of the inertia of the constraining layer is neglected, it can be shown that the following closed form solutions satisfy both equations (9) and (10) as well as the boundary conditions given by equations (11a) and (11b):

$$u - u_0 = (\varepsilon_{px} - \varepsilon_{0x})\, B_x^* \sinh(x/B_x^*)/\cosh(a/2B_x^*) \tag{17}$$

and

$$v - v_0 = (\varepsilon_{py} - \varepsilon_{0y})\, B_y^* \sinh(y/B_y^*)/\cosh(b/2B_y^*) \tag{18}$$

Note that when $\epsilon_{px} = 0$, equation (17) reduces to Plunkett and Lee's result. Substitution of equations (17) and (18) into equation (15) leads to

$$\epsilon_{px} = \epsilon_{0x} \cdot \frac{2K_x\,\omega B_x\, b[\tanh(A) - A + (a/b)\,(\varepsilon_{0y}/\varepsilon_{0x})\,(K_y/K_x)\,(B_y^*/B_x^*)\{\tanh(B) - B\}]}{1 + 2K_x\,\omega B_x\, b\{\tanh(A) + (a/b)\,(K_y/K_x)\,(B_y^*/B_x^*)\,(d_{32}/d_{31})\,tanh\,(B)\}}, \tag{19}$$

wherein $A = a/2B_x^*$ and $B = b/2B_y^*$.

Implementation of the control strategy requires that the piezo-actuator must be designed as an actuator with self-sensing capabilities in the x and y directions using the approaches suggested by Dosch, *et al*. [25]. It is important also to note that the temporal derivatives of u and v can be determined by monitoring the current of the piezo-sensor rather than its voltage as described, for example, by Miller and Hubbard [26].

5. ENERGY DISSIPATION CHARACTERISTICS OF THE ACLD AND PCLD TREATMENTS

5.1. ENERGY DISSIPATION PER VIBRATION CYCLE

The energy dissipation characteristics of the ACLD is quantified by using equation (13) to calculate the energies, ΔW_{pa} and ΔW_a, which are dissipated per vibration cycle by the passive and active components of the ACLD treatment, respectively, as follows:

$$\Delta W_{pa} = (G'\eta_g\, h_1/\omega) \int_0^{2\pi/\omega} \int_{-b/2}^{b/2} \int_{-a/2}^{a/2} (\gamma_{1t}^2 + \gamma_{2t}^2)\, \mathrm{d}x\, \mathrm{d}y\, \mathrm{d}t \tag{20}$$

and

$$\Delta W_a = \int_0^{2\pi/\omega} h_2 \left[\int_{-b/2}^{b/2} (C_{11}\,\varepsilon_{px} + C_{12}\,\varepsilon_{py})\{u_t(a/2) - u_t(-a/2)\}\, \mathrm{d}y \right.$$

$$\left. + \int_{-a/2}^{a/2} (C_{12}\,\varepsilon_{px} + C_{22}\,\varepsilon_{py})\{v_t(b/2) - v_t(-b/2)\}\, \mathrm{d}x \right] \mathrm{d}t, \tag{21}$$

where $2\pi/\omega$ is the period of an excitation.

Use of equations (1) and (15) through (18), reduces equations (20) and (21) to

$$\Delta W_{pa} = \pi G' \eta_g / h_1 \left[b\varepsilon_{0x}^2 (\varepsilon_{px}/\varepsilon_{0x} - 1)^2 B_x^2 \int_{-a/2}^{a/2} \times [|\sinh(x/B_x^*)/\cosh(a/2B_x^*)|]^2 \, \mathrm{d}x + a\varepsilon_{0y}^2 (\varepsilon_{py}/\varepsilon_{0y} - 1)^2 B_y^2 \int_{-b/2}^{b/2} [|\sinh(y/B_y^*)/\cosh(b/2B_y^*)|]^2 \, \mathrm{d}y \right] \quad (22)$$

and

$$\Delta W_a = 4\pi b^2 h_2 \, \omega K_x B_x^2 (C_{11} + (d_{32}/d_{31}) C_{12}) |[(\varepsilon_{px}/\varepsilon_{0x} - 1)\tanh(A) + A + (a/b)(\varepsilon_{0y}/\varepsilon_{0x})(K_y/K_x)(B_y^*/B_x^*)\{(\varepsilon_{py}\varepsilon_{0x} - 1)\tanh(B) + B\}]|\varepsilon_{px}\varepsilon_{0x}, \quad (23)$$

where, B_x and B_y are the magnitudes of the complex characteristic length, B_x^*, and breadth, B_y^*, respectively.

5.2. LOSS COEFFICIENTS: PASSIVE, ACTIVE AND TOTAL

Now, following Plunkett and Lee [18] the nominal energy, W_n, for the PCLD treatments may be defined as

$$W_n = \tfrac{1}{2} \, \mathrm{abh}_2 \, \varepsilon_{0x}^2 \, C_{11} [1 + 2(C_{12}/C_{11})(\varepsilon_{0y}/\varepsilon_{0x}) + (C_{22}/C_{11})(\varepsilon_{0y}^2/\varepsilon_{0x}^2)] \quad (24)$$

to denote the maximum strain energy of the constraining layer if the whole layer is subjected to uniform longitudinal strains, ε_{0x} and ε_{0y}, only in x and y directions, respectively. Then, equations (22) and (23) can be normalized with respect to the nominal energy given by equation (24) to give the dimensionless loss coefficients, η_{pa} and η_a, that quantify the energies dissipated by the passive and active components of the ACLD treatment as

$$\eta_{pa} = \frac{4\pi}{1 + 2(C_{12}/C_{11})(\varepsilon_{0y}/\varepsilon_{0x}) + (C_{22}/C_{11})(\varepsilon_{0y}^2/\varepsilon_{0x}^2)} \left[\left(\frac{\varepsilon_{px}}{\varepsilon_{0x}} - 1 \right)^2 \times \frac{D\sinh(Cw_x) - C\sin(Dw_x)}{w_x\{\cosh(Cw_x) + \cos(Dw_x)\}} + \frac{C_{22}}{C_{11}} \frac{\varepsilon_{0y}^2}{\varepsilon_{0x}^2} \left(\frac{\varepsilon_{py}}{\varepsilon_{0y}} - 1 \right)^2 \frac{D\sinh(Cw_y) - C\sin(Dw_y)}{w_y\{\cosh(Cw_y) + \cos(Dw_y)\}} \right] \quad (25)$$

and

$$\eta_a = \frac{8\pi(1 + (d_{32}/d_{31})(C_{12}/C_{11}))}{1 + 2(C_{12}/C_{11})(\varepsilon_{0y}/\varepsilon_{0x}) + (C_{22}/C_{11})(\varepsilon_{0y}^2/\varepsilon_{0x}^2)} \times \left| \frac{K_x \omega B_x^* b[\tanh(A) - A + (a/b)(\varepsilon_{0y}/\varepsilon_{0x})(K_y^*/K_x^*)(B_y/B_x)\{\tanh(B) - B\}]}{w_x[1 + 2K_x \omega B_x^* b\{\tanh(A) + (a/b)(K_y/K_x)(B_y^*/B_x^*)(d_{32}/d_{31})\tanh(B)\}]} \right|$$

$$\times \left| (\varepsilon_{px}/\varepsilon_{0x} - 1)\tanh(A) + A + (a/b)(\varepsilon_{0y}/\varepsilon_{0x})(K_y/K_x)(B_y^*/B_x^*) \right.$$

$$\left. \times \left\{ \left(\frac{\varepsilon_{py}}{\varepsilon_{0y}} - 1 \right) \tanh(B) + B \right\} \right|, \tag{26}$$

where $w_x = a/B_x$, $w_y = b/B_y$, $C = \cos(\theta/2)$ and $D = \sin(\theta/2)$. Therefore, equations (25) and (26) provide closed-form expressions of the loss coefficients, η_{pa} and η_a, as functions of dimensionless parameters θ, w_x, $(K_x \omega B_x b)$ and a/b. These parameters define the loss factor of the viscoelastic layer ($\theta = \tan^{-1}\eta_g$), a dimensionless length of the constraining layer, dimensionless control gain and aspect ratio of the plate, respectively. The sum of these two equations give the total loss coefficient η_t of the ACLD treatment due to the combined passive and active components as

$$\eta_t = \eta_{pa} + \eta_a. \tag{27}$$

Note that in the case of PCLD, the expressions for η_{pa} (equation 25) reduces to that of Plunkett and Lee [18] if $\varepsilon_{px} = \varepsilon_{py} = 0$, $K_x = K_y = 0$ and $\varepsilon_{0y} = 0$.

It is important here to note that the loss coefficients η_{pa} and η_a are not loss factors because the normalization of the energy dissipated is done with respect to a nominal structural energy rather than the actual structural energy.

In section 6, equations (25)–(27) are utilized to select the optimal dimensionless length ($w_x = a/B_x$) and control gain ($K_x \omega B_x b$) of ACLD treatments for different loss factors (η_g) and aspect ratio (a/b) in order to maximize the total loss coefficient, η_t.

6. OPTIMIZATION OF ENERGY DISSIPATION OF THE ACID TREATMENT

6.1. OVERVIEW

Extensive efforts have been exerted to optimally design passive and active constrained layer damping treatments of vibrating structures. For the PCLD treatments, these efforts aim primarily at maximizing the modal damping ratios, modal strain energies or energy dissipation coefficients and/or minimizing the weight by selecting the optimal length [18, 19, 27, 28] optimal location [29] and/or optimal material and geometrical parameters of the treatments [30–32]. Recently, attempts have been made to optimize the performance of the ACLD treatments by selecting the optimal thickness and shear modulus of the viscoelastic cores as well as the control gains for fully-treated beams when proportional and derivative controllers are used [8, 17]. Also, Baz [5] determined the optimal length and control gains for ACLD treatments of beam-type structures by maximizing the sum of the passive and active loss coefficients.

In this study, the optimal length and control gain of the ACLD treatments are selected for different aspect ratios (a/b) and loss factors (η_g) in order to maximize the total loss coefficient η_t.

6.2. OPTIMIZATION OF THE OPEN-LOOP CHARACTERISTICS OF THE ACLD

The optimization problem of the energy dissipation characteristics of the ACLD is first formulated to optimize the energy dissipation characteristics of the open-loop ACLD treatment, i.e., the PCLD treatment. Such a problem for the PCLD treatment may be described mathematically as

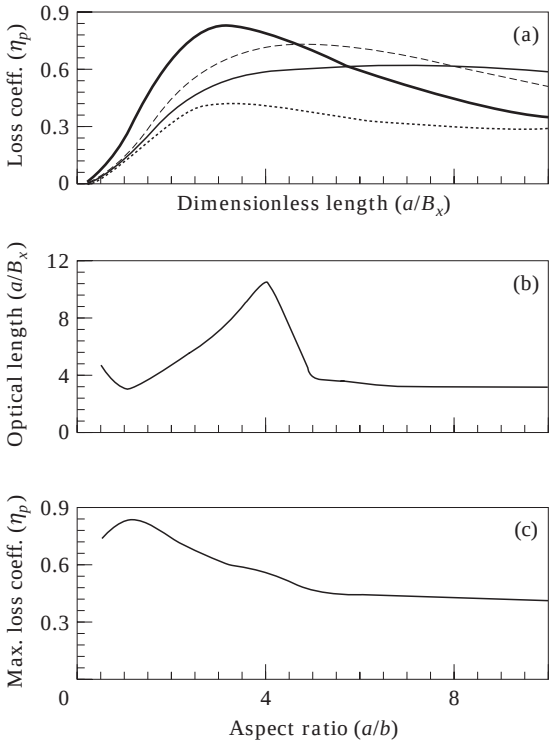

Figure 4. Optimal solutions for open loop ACLD treatment. (a) Variation of passive loss coefficient (η_{pa}) with dimensionless length (a/B_x) for various aspect ratios (a/b) and $\eta_g = 1$; ——, $a/b = 1$;---, 2; —, 3; . . . , 10. (b) Variation of optimal length (a/B_x) with aspect ratio (a/b) for $\eta_g = 1$. (c) Variation of maximum passive loss coefficient (η_{pa}) with aspect ratio (a/b) for $\eta_g = 1$.

$$\begin{gathered}\text{Find the length } w_x \\ \text{to maximize the total loss coefficient } \eta_t \\ \text{such that the loss factor } \eta_g \text{ is known,} \\ \text{aspect ratio } a/b \text{ is known} \\ \text{and gain } K_x\, \omega B_x\, b = 0\end{gathered} \tag{28}$$

In this manner, the treatment is designed initially to provide the maximum energy dissipation when it is in its open-loop mode. This guarantees the robustness of operation of the ACLD treatment in the case of failure of the controller when it is in its closed-loop mode. Numerical solutions are sought considering the material of the piezo-constraining layer as elastically isotropic so that $C_{11} = C_{22}$ when $\varepsilon_{0x} = \varepsilon_{0y}$, and Poisson's ratio ($C_{12}/C_{11}$) is 0·33.

Figure 4(a) shows the optimal solutions for open-loop ACLD treatments for various aspect ratios (a/b) with $\eta_g = 1$. It can be observed from this figure that the aspect ratio plays a significant role on the optimal solutions. For example, the optimum length of the constraining layer increases as the aspect ratio increases from 1 to 3 and then decreases with further increase in the aspect ratio as shown in Figures 4(a) and 4(b). However, the maximum loss coefficient decreases monotonically with the aspect ratio as indicated in Figure 4(c). The optimal length of the PCLD treatment remains nearly independent of the

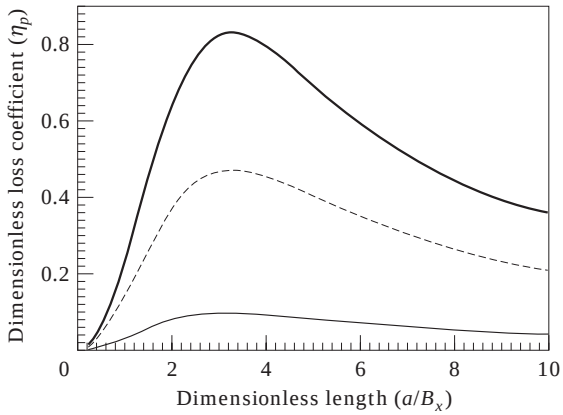

Figure 5. Effect of length (a/B_x) on passive loss coefficient (η_{pa}) for different visco-elastic material loss factors; —, $\eta_g = 1{\cdot}0$; ---, $0{\cdot}5$; —, $0{\cdot}1$.

loss factor η_g of the viscoelastic layer [18, 19] as shown in Figure 5 for $a/b = 1$. The results, displayed in Figures 4 and 5, suggest that square passive treatments (with $a/b = 1$) produce the maximum loss coefficient irrespective of the viscoelastic loss factor η_g.

6.3. OPTIMIZATION OF THE CLOSED-LOOP CHARACTERISTICS OF THE ACLD

The optimum design problem of the closed-loop ACLD treatment aims at selecting the optimal control gain ($K_x\,\omega B_x\,b$) to maximize the energy dissipation characteristics of the ACLD using the optimal length for PCLD treatment. It is formulated as

$$\begin{gathered}\text{Find gain } (K_x\,\omega B_x\,b)\\ \text{to maximize the total loss coefficient } \eta_t\\ \text{such that the loss factor } \eta_g \text{ is known}\\ \text{and } a/B_x = \text{optimal length of PCLD}\end{gathered} \tag{29}$$

Figures 6 and 7 show the optimal solutions for closed-loop ACLD treatments for piezo-strain ratios (d_{32}/d_{31}) = 1 and $0{\cdot}130$ to simulate piezo-ceramics and piezo-polymers,

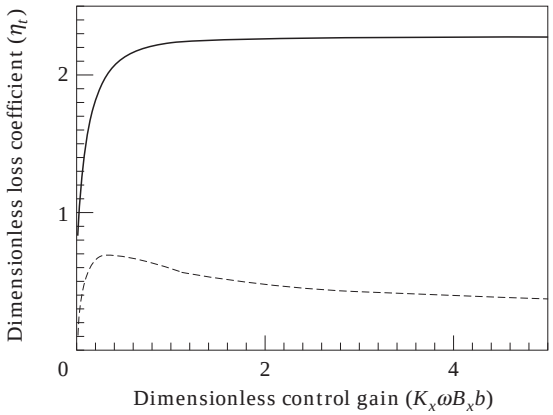

Figure 6. Effect of control gain ($K_x\omega B_x b$) on dimensionless loss coefficient (η_t) for closed loop ACLD treatment for different loss factors (η_g) with $d_{32}/d_{31} = 1$: —, $\eta_g = 1$; ---, $0{\cdot}1$.

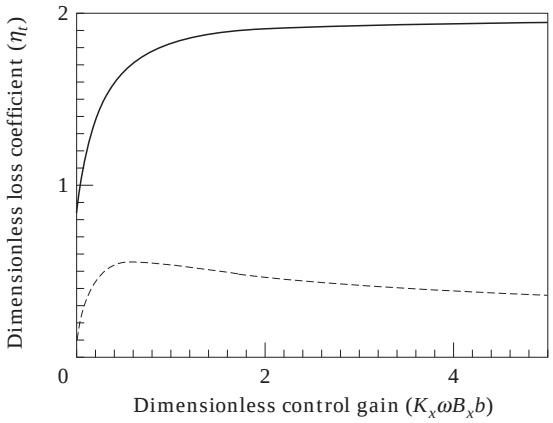

Figure 7. Effect of control gain ($K_x\omega B_x b$) on dimensionless loss coefficient (η_t) for closed loop ACLD treatment for different loss factors (η_g) with $d_{32}/d_{31} = 0{\cdot}130$: —, $\eta_g = 1{\cdot}0$; ---, $0{\cdot}1$.

respectively. The results displayed in these two figures are for $a/b = 1$, $E_{2y}/E_{2x} = 1$ and $\varepsilon_{0y}/\varepsilon_{0x} = 1$. It is clear from these figures that active control enhances considerably the energy dissipation characteristics. This is attributable to the piezoelectrically-induced strains (ε_{px} and ε_{py}) in the constraining layer and is corroborated by equations (19), (25–27). Furthermore, there is an optimal gain, for each viscoelastic material, at which the loss coefficient becomes maximum. Such optimal gain increases as the viscoelastic loss factor, η_g increases.

Figure 8 shows the improvement in the shear strain distribution inside the viscoelastic core due to the use of the optimally controlled ACLD when $\eta_g = 0{\cdot}1$. It is evident that the shear strain increases over the entire length of the treatment which in turn results in increasing the passive energy dissipation per cycle according to equation (20).

Figure 9 shows the total loss coefficient η_t at which the energy dissipation by the ACLD treatment attains its maximum as a function of the loss factor η_g of the viscoelastic core for $a/b = 1$. Displayed in this figure are also the loss coefficients of PCLD treatments for the sake of comparison. It is clear that the ACLD treatment causes remarkable improvement of the energy dissipation characteristics as compared to that of the PCLD particularly when the loss factor η_g of the viscoelastic core is small. For example, the ratio

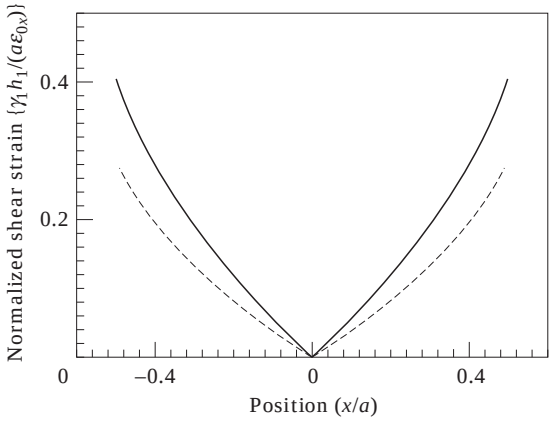

Figure 8. Comparison between the shear strain distributions of the ACLD (—) and PCLD (---) treatments for $\eta_g = 0{\cdot}1$, $d_{32}/d_{31} = 1$ and $K_x\omega B_x b = 0{\cdot}35$.

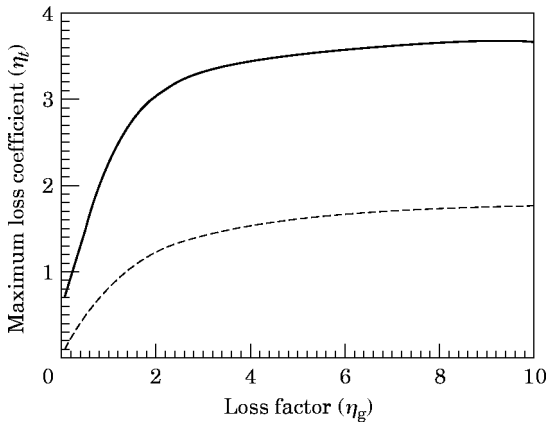

Figure 9. Comparison between the effect of visco-elastic material loss factors (η_g) on the maximum loss coefficients (η_t) of ACLD (—) and PCLD (---) treatments for $a/b = 1$ and $d_{32}/d_{31} = 1$.

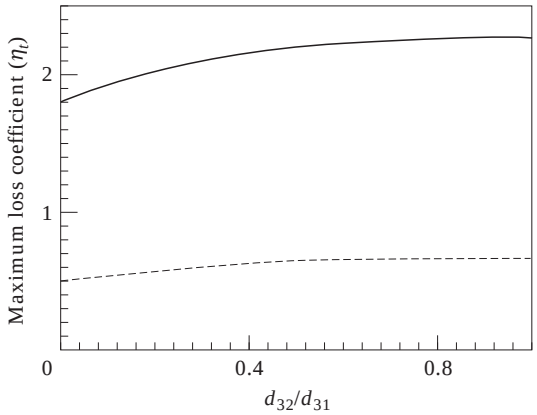

Figure 10. Effect of the ratio of piezo-electric constants (d_{32}/d_{31}) on the maximum loss coefficient (η_t) for different loss factors (η_g) with $a/b = 1$: —, $\eta_g = 1{\cdot}0$; ---, $0{\cdot}1$.

between the maximum value of η_t of the ACLD treatment to that of the PCLD is about $7{\cdot}8$ when $\eta_g = 0{\cdot}1$ and becomes $2{\cdot}8$ when $\eta_g = 1$. Note that small η_g means θ which, in turn, implies that the viscoelastic core is stiff and as manifested by the storage modulus $G' = G\cos\theta$ with G remaining constant for a given B_x. Hence, ACLD with stiffer viscoelastic cores are more effective than treatments with softer cores provided that the thickness and length of the core are maintained constant.

Figure 10 demonstrates the effect of the ratio of the piezoelectric constants, d_{32}/d_{31}, on the performance of the ACLD treatment for different loss factors when $a/b = 1$. It is evident that the active damping of the piezo-constraining layer increases as the anisotropy of the piezoelectrical properties of the constraining layer decreases. Hence, constraining layers made of piezo-ceramics (d_{32}/d_{31}) significantly improve the damping characteristics of the ACLD treatment as compared to layers made of piezo-polymers ($d_{32}/d_{31} = 0{\cdot}130$).

7. CONCLUSIONS

This paper has extended the pioneering and ingenious work of Plunkett and Lee [18] for finding the optimal length of PCLD treatments, to optimize the performance of ACLD

treatments of plate. In the present study, the optimal size and control gains are determined to maximize the energy dissipation of the ACLD treatments. Such optimization is based on developing a variational formulation of the dynamics of the ACLD treatments and devising a globally stable boundary control strategy which is compatible with the operating nature of the ACLD treatment. Closed-form expressions of the passive, active and total loss coefficients have been developed and used in the formulation of the optimal design problems of the ACLD treatment. Solutions of the optimization problem of the open-loop ACLD treatment provided the optimal size of the treatment and solutions of the optimal closed-loop ACLD problem yielded the optimal control gains. Such solutions for optimal size of the ACLD treatment guarantees the robustness of its operation in case of failure of the controller when it is in its closed-loop mode. The effect of the aspect ratio (a/b) and the loss factor of the viscoelastic core on the optimal solutions have been studied. It is found that the ACLD treatment performs better at the cost of robustness of the controller when the constraining actuating layer becomes rectangular in shape. The effect of the loss factor on the optimal solutions establishes that ACLD treatment is more effective in dissipation of energy with a stiff viscoelastic core than with a softer core. Also, it is found that the performance of the ACLD treatment increases as the anisotropy of the piezoelectrical properties of the constraining layer decreases. It is important to note here that, as with Plunkett and Lee [18], the present study is based on the basic assumption that ε_{0x} and ε_{0y} are constant. Extension of the present paper can be easily performed to include other strain distributions such as the linearly varying strain assumption of Demoret and Torvik [19].

ACKNOWLEDGMENTS

Part of this work is funded by the U.S. Army Research Office (Grant number DAAH-04-93-G-0202). Special thanks are due to Dr. Gary Anderson, the technical monitor, for his invaluable technical inputs.

REFERENCES

1. G. S. Agnes and K. Napolitano 1993 *Proceedings of 34th SDM Conference*, 3499–3506. Active constrained layer viscoelastic damping.
2. B. Azvine, G. Tomlinson and R. Wynne 1994 *Proceedings of Smart Structures and Materials Conference on Passive Damping*, (editor, C. Johnson) Orlando, Florida. **2193**, 138–149. Initial studies into the use of active constrained-layer damping for controlled resonant vibrations.
3. I. Y. Shen 1994 *American Society of Mechanical Engineers Journal of Vibration and Acoustics* **116**, 341–349. Hybrid damping through intelligent constrained layer treatments.
4. A. Baz 1996 *U. S. Patent* 5485 053. Active constrained layer damping.
5. A. Baz 1996 *Journal of Smart Materials and Structures*. Optimization of energy dissipitation characteristics of active constrained layer damping.
6. A. Baz *DAMPING*'93 *Conference*, San Francisco, CA, February, IBB 1–23. Active constrained Layer Damping.
7. A. Baz 1995 *American Society of Mechanical Engineers Journal of Vibration and Acoustics*. Boundary control of beams using active constrained layer damping.
8. A. Baz 1995 *Tenth VPI & SU Conference on Dynamics & Control of Large Structures*, Blacksburg, VA. Dynamic boundary control of beams using active constrained layer damping.
9. A. Baz and J. Ro 1993 *Conference of Engineering Science Society*, *ASME-AMD* **67**, 61–80, Charlottesville, VA, Partial treatment of a flexible beam with active constrained layer damping.
10. A. Baz and J. Ro 1993 *Ninth VPI & SU Conference on Dynamics & Control of Large Structures*, Blacksburg, VA. pp. 345–358. Finite element modeling and performance of active constrained layer damping.
11. A. Baz and J. Ro 1994 *Sound & Vibration Magazine* **28**, 18–21. Actively controlled constrained layer damping.

12. A. Baz and J. Ro 1995 *Shock and Vibration Journal* **2**, 33–42. Performance characteristics of active constrained layer damping.
13. A. Baz and J. Ro 1995 *American Society of Mechanical Engineers Journal of Vibration and Acoustics*, **117**B, 135–144. Optimum design and control of active constrained layer damping.
14. D. Edberg and A. Bicos 1992 *Conference on Active Materials and Adaptive Structures* (editor G. Knowles) IOP Publishing Ltd., Bristol, UK, 377–382. Design and development of passive and active damping concepts for adaptive structures.
15. J. Plump and J. E. Hubbard 1986 *Twelvth International Congress on Acoustics*, Paper D41, Toronto, Canada, 24–31. Modeling of an active constrained layer damper.
16. W. Van Nostrand, G. Knowles and D. Inman 1994 *Proceedings of Smart Structures and Materials Conference on Passive Damping* (editor C. Johnson) Orlando, Florida, **2193**, 126–137, Finite element modeling for active constrained-layer damping.
17. M. Liao and K. Wang 1995 *American Society of Mechanical Engineers Design Engineering Technical Conference*, Boston, MA, **84–3**, 125–141. On the active–passive hybrid vibration control actions of structures with active constrained layer treatments.
18. R. Plunkett and C. T. Lee 1970 *Journal of Acoustical Society of America* **48**, 150–161. Length optimization for constrained viscoelastic layer damping.
19. K. Demoret and P. Torvik 1995 *Proceedings of American Society of Mechanical Engineers Design Engineering Technical Conference*, Boston, MA, DE **83–3**, 719–726. Optimal length of constrained layers on a substrate with linearly varying strains.
20. A. Nashif, D. I. Jones and J. P. Henderson 1985 *Vibration Damping*. New York: John Wiley.
21. M. J. Lam, W. R. Saunders and D. J. Inman 1995 *Smart Structures and Materials Conference*, San Diego, CA, 2445–09. Modeling active constrained layer damping using finite element analysis and GHM damping approach.
22. L. Meirovitch 1967 *Analytical Methods in Vibrations*, New York: Macmillan.
23. A. G. Butkovskiy 1969 *Distributed Control Systems*. New York: Elsevier Publishing.
24. I. Y. Shen 1995 *Proceedings of American Society of Mechanical Engineers Design & Engineering Technical Conference* Boston, MA, DE **84–3**, 149–160. A variational formulation: a work-energy relation and damping mechanisms of active constrained layer treatments.
25. J. J. Dosch, D. J. Inman and E. Garcia 1992 *Journal of Intelligent Material Systems and Structures* **3**, 166–184. A self-sensing piezoelectric actuator for collocated control.
26. S. Miller and J. Hubbard, Jr. 1987 *Seventh Conference on Dynamics & Control of Large Structures*, VPI & SU, Blacksburg, VA, 375–930. Observability of a Bernoulli–Euler beam using PVF_2 as a distributed sensor.
27. W. Gibson and C. Johnson 1987 *The Role of Damping in Vibration and Noise Control* (editors L. Rogers and J. C. Simonis) *American Society of Mechanical Engineers DE* 5, 143–149. Optimization methods for design of viscoelastic damping treatments.
28. T. E. Alberts, Y. Chen and H. Xia 1990 *Advances in Optical Structure System*, SPIE **1303**, 274–285. On the effectiveness of section length optimization for constrained viscoelastic layer damping treatment.
29. Raju Mantena, P. R. Gibson and S. Hwang, 1991 *American Institute of Aeronautics and Astronautics Journal* **29**, 1678–1685. Optimal constrained viscoelastic tape lengths for maximizing damping in laminated composites.
30. D. K. Rao 1976 *American Society of Mechanical Engineers Journal of Engineering for Industry* **98**, 391–396. Static response of stiff-cored unsymmetric sandwich beams.
31. T. E. Alberts and H. Xia 1995 *American Society of Mechanical Engineers Journal of Vibration and Acoustics* **117**, 398–404. Design and analysis of fiber enhanced viscoelastic damping polymers.
32. S. Kodiyamalam and J. Molnar 1992 *American Institute of Aeronautics and Astronautics paper* 92-2269-CP. Optimizaton of constrained viscoelastic damping treatments for passive vibration control.